References and Notes

1. C. U. Hammer, H. B. Clausen, W. Dansgaard, *Nature (London)* **288**, 230 (1980). Some of these acidity peaks have been confirmed by M. M. Herron [*J. Geophys. Res.* **87**, 3052 (1982)].
2. H. H. Lamb, *Philos. Trans. R. Soc. London Ser. A* **266**, 425 (1970). Lamb's "dust veil index" characterizing large volcanic eruptions has been correlated with Greenland acidity peaks over the period A.D. 1770 to 1972 [C. U. Hammer, *Nature (London)* **270**, 482 (1977)].
3. H. Sigurdsson, *Eos* **63**, 601 (1982).
4. W. A. Petroeschevsky, *Tijdschr. K. Ned. Aardrijksk. Genoot.* **66**, 688 (1949); J. D. Post, *The Last Great Subsistence Crisis in the Western World* (Johns Hopkins Univ. Press, Baltimore, 1977); H. Stommel and E. Stommel, *Sci. Am.* **240**, 176 (June 1979).
5. J. W. Judd, "The eruption of Krakatoa and subsequent phenomena," part 1, *Report of the Krakatoa Committee of the Royal Society*, G. J. Symons, Ed. (Treubner, London, 1888); A. Heilprin, *The Eruption of Pelée* (Lippincott, Philadelphia, 1908).
6. R. B. Stothers and M. R. Rampino, *J. Geophys. Res.*, in press. For the period 735 B.C. to A.D. 630, our search of European and Near Eastern literature was intended to be complete except within a few genres (for example, medicine, astrology, grammar, rhetoric, and religion) where extensive sampling turned up little relevant material; the equivalent of about one quarter of a million pages of modern English text was examined.
7. The effects of the eruption lasted 3 years and were observed also in China; the *Han shu* records (for May to June 43 B.C.): "The sun's color was pale blue and there were no shadows (on the ground). At noon exactly there were shadows but no brightness." The translation is taken from D. H. Clark and F. R. Stephenson, *Q.J.R. Astron. Soc.* **19**, 387 (1978).
8. C. U. Hammer (personal communication) reported that the relative accuracy of his assigned ice-core dates within this 195-year section of the record is ±5 years and probably much better.
9. G. Kieffer, *C. R. Acad. Sci.* **288**, 1023 (1979).
10. G. Wadge and J. E. Guest, *Nature (London)* **294**, 548 (1981).
11. R. D. Cadle, C. S. Kiang, J.-F. Louis, *J. Geophys. Res.* **81**, 3125 (1976); K. A. Rahn, E. Joranger, A. Semb, T. J. Conway, *Nature (London)* **287**, 824 (1980).
12. C. U. Hammer *et al.*, *J. Glaciol.* **20**, 3 (1978); C. U. Hammer, *ibid.* **25**, 359 (1980); M. Maccagnan, J. M. Barnola, R. Delmas, P. Duval, *Geophys. Res. Lett.* **8**, 970 (1981).
13. We have inferred this from the eruption statistics in T. Simkin, L. Siebert, L. McClelland, D. Bridge, C. Newhall, J. H. Latter [*Volcanoes of the World* (Hutchinson Ross, Stroudsburg, Pa., 1981)]. The statement is supported by studies of longer time scales; see, for example, J. R. Hein, D. W. Scholl, J. Miller, *Science* **199**, 137 (1978); R. A. Bryson and B. M. Goodman, *ibid.* **207**, 1041 (1980).
14. A. T. Anderson, *Geol. Soc. Am. Bull.* **85**, 1485 (1974); D. R. Haughton, P. L. Roeder, B. J. Skinner, *Econ. Geol.* **69**, 451 (1974); M. R. Rampino and S. Self, *Quat. Res. (N.Y.)* **18**, 127 (1982).
15. G. S. Gorshkov, *Bull. Volcanol.* **20**, 77 (1959); S. N. Williams and S. Self, *J. Volcanol. Geotherm. Res.*, in press.
16. We thank the two referees for their helpful comments on the manuscript and C. U. Hammer for supplying detailed copies of his acidity records and for a valuable discussion. Supported in part by a NASA grant to Columbia University.

2 September 1982; revised 10 February 1983

Rates of Hydrothermal Reactions

Abstract. *The rates of reactions of silicates and aqueous fluids follow zero-order kinetics controlled by the reacting surface area with the rate constant given by the equation:* $\log k \simeq -2900/T - 6.85$, *where* T *is temperature and where* k *has the unit's gram-atoms of oxygen per square centimeter per second. This expression appears to hold for all silicates and for reactions involving dissolution, fluid production, or solid-solid transformations in the presence of a fluid of moderate to high* pH.

The rate relations of hydrothermal reactions are of considerable interest in geologic and materials sciences. A full understanding of these processes would enable us to predict weathering phenomena, reactions in geothermal and metamorphic systems, and the aqueous dissolution behavior of, for example, nuclear waste–bearing ceramics. In the course of reviewing published data (*1–19*) on reaction rates, we have discovered a general Arrhenius relation between reaction rate and temperature that appears to hold over temperatures from 25° to 710°C. It also holds for a large number of different silicate and related mineral species.

In the most detailed studies of mineral reaction rates (*1–7*), investigators have examined low-temperature dissolution phenomena of the type associated with weathering at the earth's surface. Such reactions may be represented as follows:

$$\text{mineral} + H_2O \rightarrow \text{aqueous solution} + \text{secondary solids} \qquad (1)$$

Although many experimenters have found complex dissolution behavior, it has recently been shown (*4, 20, 21*) that apparent nonlinear relations are artifacts of sample preparation. Once fine-grained material is removed, dissolution follows a zero-order rate relation (*3–7*) controlled by the reacting surface area:

$$\frac{dm}{dt} = k_{\mathrm{dis}} \qquad (2)$$

The rate of removal of mass from the dissolving mineral (dm/dt, in moles per square centimeter per second) is therefore a constant at fixed temperature, pressure, and activities of solution species. The rate constant, k_{dis}, is, however, a function of temperature (*1, 7, 21*) and is *p*H-dependent in acidic solutions. Dissolution rates increase with increasing temperature (*1*) and with decreasing *p*H. At moderate to high *p*H [> 5 for feldspar at 25°C (*4, 20*)], however, the dissolution rate becomes *p*H-independent. The reason for the change in behavior reflects the nature of the rate-determining step. At high activities of H_3O^+ the hydrolysis process involves H_3O^+ in the rate-determining step, whereas at very low activities of this species undissociated solvent (H_2O) is the agent of hydrolysis (*20*). The extent of the *p*H-dependent region varies from phase to phase (*4, 20, 21*), presumably because of different interfacial properties and extents of H_3O^+ adsorption.

Most dissolution experiments have been performed in the temperature range from 0° to 90°C, with a few studies (*1, 2, 7*) extending up to 300°C. The higher temperature experiments were predominantly directed toward establishing equilibrium rather than toward estimating kinetic properties of reactions. Many of these "equilibrium" studies may be used to estimate reaction rates, provided certain assumptions are made about the nature of the rate-controlling process.

Let us consider a generalized high-temperature reaction involving solid and fluid phases:

$$\text{phase A} + \text{phase B} = \text{phase C} + \text{phase D} \qquad (3)$$

Such reactions are generally studied in order to establish the temperature and pressure conditions of equilibrium between phases A, B, C, and D, one of which is typically a fluid. One of the most precise and successful methods of determining equilibrium in such cases (*8–19, 22*) is to use a fine-grained matrix of all but one of the product and reactant solids and a single crystal of the remaining phase. The experimental method requires only a few percent of fluid so that the production of fluid species is minimized. One then determines the direction of reaction by weighing the single crystal before and after the experiment to determine whether it is in the stable or unstable assemblage (Fig. 1). This method yields equilibrium at the point of zero weight change and, near equilibrium, an approximately linear relation between weight change and temperature (Fig. 1) (*23*). Linear behavior close to equilibrium is predicted by transition state theory (*20, 23–25*) which, under these circumstances, yields an equation of the form

$$\frac{dm}{dt} = \frac{k_r\,[\Delta S_r(T - T_{\mathrm{eq}})]}{RT_{\mathrm{eq}}} \qquad (4)$$

where k_r is the rate constant for the forward reaction at the equilibrium temperature T_{eq} (in kelvins), ΔS_r is the overall entropy change of the reaction, and R is the gas constant. Using Eq. 4, we have extracted k_r values for a large number of single-crystal studies (*8–19*) performed at temperatures from 300° to 710°C (Fig. 2). Values of ΔS_r were computed from data of Helgeson *et al.* (*26*). Values of ΔS_r for reactions in H_2O–CO_2 were corrected for nonideal fluid behavior. The linear approximation breaks down far from equilibrium because of the temperature dependence of k_r (*23*) (Fig. 1). Nevertheless, the linear portion generally spans a wide enough temperature range to permit estimation of k_r within a factor of 2 (Fig. 2).

In order to compare the widely differing studies, we found it necessary to make some assumptions about the rate-determining steps that controlled the rates of weight change. Because the surface area of the single crystal is relatively small (~ 0.5 cm^2) relative to the other fine-grained phases and because the presence of a fluid provides an abundant medium for diffusion, we assumed that the rate of surface reaction at activated sites on the single crystal is rate-determining. This applies for either growth or dissolution of the single crystal. Thus, given approximate crystal masses, geometries, and hence surface areas by the various researchers, we cast Eq. 4 to yield (dm/dt) in terms of moles per square centimeter per second. In order to compare studies with different minerals, we normalized each rate constant to gram-atoms of oxygen per square centimeter per second (Fig. 2), that is, we multiplied each molar rate by the number of oxygens per mole. Although the grain size of the powdered material has some effect on the rate (*9*), we assumed that this was of second order since it appears to be less than a factor of 3 (*9*).

The assumption of surface reaction control is vindicated by the consistency between k_r values derived from different studies (Fig. 2). These values show an Arrhenius temperature dependence with relatively little scatter and no consistent difference between different mineral species. This result implies that the k_r of surface reaction for a wide range of silicates (and for corundum) is similar at any fixed temperature.

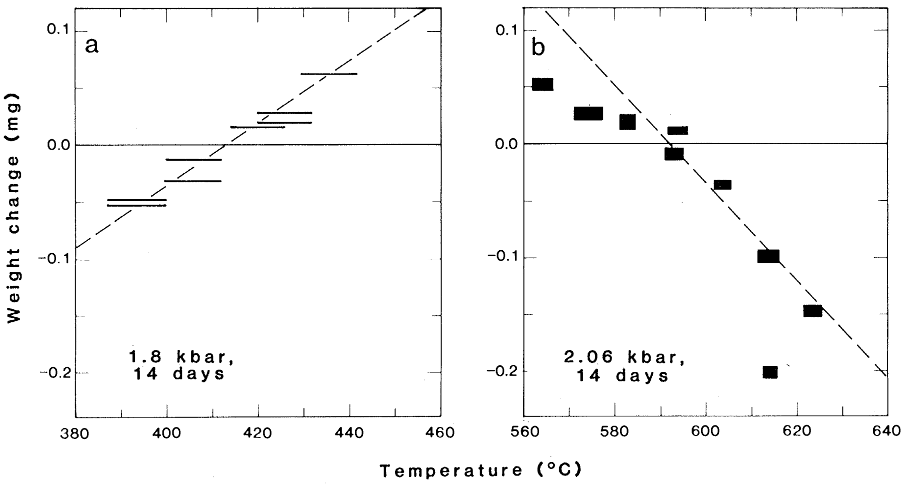

Fig. 1. (a) Weight changes of single crystals of quartz for the reaction pyrophyllite = andalusite + 3 quartz + H_2O (*11*). (b) Weight changes of single crystals of clinozoisite for the reaction 4 clinozoisite + quartz = grossularite + 5 anorthite + 2 H_2O (*10*).

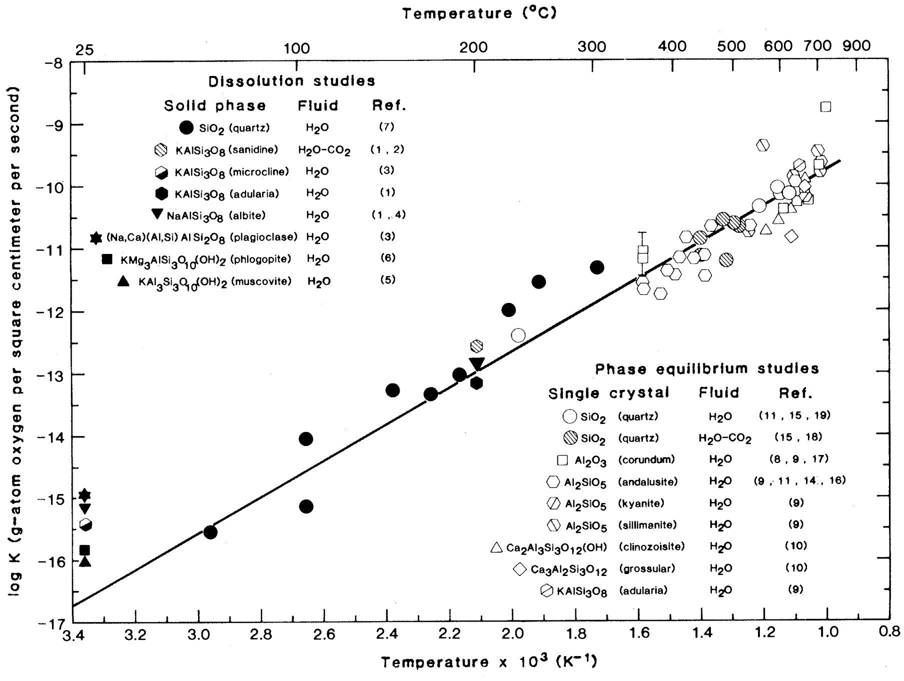

Fig. 2. Arrhenius plot of the reciprocal of absolute temperature ($1/T$) versus the logarithm (to the base 10) of the rate constant, determined from both dissolution and phase-equilibrium studies.

A final test of the hypothesis of surface-reaction control of the hydrothermal reactions is provided by the low-temperature dissolution data. If, as suggested here, surface detachment (or attachment) is rate-controlling, then from transition state theory (*20, 23*) k_{dis} in Eq. 2 (corrected to gram-atoms of oxygen) and k_r in Eq. 4 should, under the same conditions, be equivalent. Figure 2 shows available dissolution data for conditions of near-neutral pH where the rates are not substantially pH-dependent (*4, 20, 27*). The available dissolution data for this particular pH regime are consistent with an extrapolation of the high-temperature "reaction rate" data, confirming our hypothesis of surface-reaction control.

In this set of studies (Fig. 2), the experimental temperature of most of the scattered and inconsistent data is 25°C, a temperature at which the crystals must be fine-grained (< 120 mesh) in order for dissolution to proceed at readily measurable rates. Grinding crystals to this size introduces substantially increased surface defects and very fine particles (*4*), which dissolve more rapidly than the bulk equilibrium surface. Etching to remove these high-surface-energy phenomena (*4*) probably also results in enhanced dissolution rates because this process produces etch pits and a thin leached layer (*27*). Thus, most of the 25°C data refer to abnormally high exposures of defects or leached-layer phenomena, whereas the higher temperature, single-crystal experiments and most of the high-temperature dissolution experiments involve cleaved (unground) crystals (*7*) with minimized concentrations of surface defects. Despite these uncertainties, the data in Fig. 2 exhibit remarkable consistency throughout the temperature range of interest.

In contrast to the case at 25°C, fluid composition appears to have little effect in the high-temperature regime. A number of the single-crystal experiments (*18*) (Fig. 2) were performed in H_2O–CO_2 fluids with up to 0.95 mole fraction of CO_2. The rates for these reactions are indistinguishable from those in pure H_2O. This finding suggests either that the rate-controlling step does not involve solvation or that H_2O partitions so strongly into the mineral interface that its concentration at the interface is not greatly affected by 95 percent dilution in the bulk of the fluid. In either case, the result greatly extends the applicability of the observed rate relation. A similar conclusion applies to the effect of total pressure; we find no systematic effect of total pressure on rate constants at pressures from 1 to 7000 bar. Thus, it appears that temperature dominates over fluid composition and pressure effects in the single-crystal studies.

The solid line in Fig. 2 describes a rate constant given by the equation

$$\log k \simeq -2900/T - 6.85 \tag{5}$$

where T is temperature and where k has the units gram-atoms of oxygen per square centimeter per second. The possible applications of this expression to geologic phenomena are many, but let us consider as an example a prograde metamorphic dehydration reaction with $\Delta S_r = 80 \text{ J K}^{-1}$. At 500°C overstep of this reaction boundary by 1°C with 2-mm crystals would cause the reaction to go to completion in 330 years, given the presence of all phases involved. At 700°C the reaction would go to completion in 70 years. These rapid rates support the classic observation (*28*) that prograde mineral assemblages remain very close to thermodynamic equilibrium when a fluid phase is present.

BERNARD J. WOOD
JOHN V. WALTHER
Department of Geological Sciences, Northwestern University, Evanston, Illinois 60201

References and Notes

1. M. Lagache, *Bull. Soc. Fr. Mineral. Cristallogr.* **88**, 223 (1965).
2. ______, *Geochim. Cosmochim. Acta* **40**, 157 (1976).
3. E. Busenburg and C. V. Clemency, *ibid.*, p. 41.
4. G. R. Holden, Jr., and R. A. Berner, *ibid.* **43**, 1161 (1979).
5. F.-C. Lin and C. V. Clemency, *ibid.* **45**, 571 (1981).
6. ______, *Clays Clay Miner.* **29**, 101 (1981).
7. J. D. Rimstidt and H. L. Barnes, *Geochim. Cosmochim. Acta* **44**, 1683 (1980).
8. W. S. Fyfe and M. A. Hollander, *Am. J. Sci.* **262**, 709 (1964).
9. B. W. Evans, *ibid.* **263**, 647 (1965).
10. M. J. Holdaway, *ibid.* **264**, 643 (1966).
11. D. M. Kerrick, *ibid.* **266**, 204 (1968).
12. A. B. Thompson, *ibid.* **269**, 267 (1970).
13. ______, *ibid.* **271**, 72 (1971).
14. M. J. Holdaway, *ibid.*, p. 97.
15. D. M. Kerrick, *ibid.* **272**, 946 (1972).
16. H. H. Haas and M. J. Holdaway, *ibid.* **273**, 449 (1973).
17. N. D. Chatterjee and W. Johannes, *Contrib. Mineral. Petrol.* **48**, 89 (1974).
18. J. Slaughter, D. M. Kerrick, V. J. Wall, *Am. J. Sci.* **275**, 143 (1975).
19. A. B. Thompson, in *Progress in Experimental Petrology*, G. M. Biggar, Ed. (Natural Environment Research Council, London, 1976), p. 9.
20. P. Aagaard and H. C. Helgeson, *Am. J. Sci.* **282**, 237 (1982).
21. J. Schott, R. A. Berner, E. L. Sjoberg, *Geochim. Cosmochim. Acta* **45**, 2123 (1981).
22. W. S. Fyfe, *J. Geol.* **68**, 553 (1960).
23. A. C. Lasaga and G. W. Fisher, in *Kinetics of Geochemical Processes*, A. C. Lasaga and R. J. Kirkpatrick, Eds. (Mineralogical Society of America, Washington, D.C., 1981), p. 135.
24. H. Eyring, *J. Chem. Phys.* **3**, 107 (1935).
25. M. Boudart, *J. Phys. Chem.* **80**, 2869 (1976).
26. H. C. Helgeson, J. M. Delany, H. W. Nesbitt, D. K. Bird, *Am. J. Sci.* **278A**, 1 (1978).
27. R. Wollast, personal communication.
28. V. M. Goldschmidt, *Z. Anorg. Chem.* **71**, 313 (1911).
29. Supported by NSF grants EAR80-24146 and 82-12502.

17 January 1983; accepted 23 June 1983

Electron Density Distribution in the Organic Superconductor $(TMTSF)_2AsF_6$

Abstract. *Excellent crystals of* $(TMTSF)_2AsF_6$ *(TMTSF, tetramethyltetraselenafulvalene) were employed to obtain x-ray diffraction data for a determination of the electron density distribution in this organic superconductor. Electron density was observed* between *molecules in a stack of donors of an organic metal and between certain* interstack *selenium atoms of these donors.*

Certain organic molecules give rise to organic metals when converted to radical ions. (*1*). These organic solids conduct electricity preferentially in one direction, usually along the long axis of the needle-shaped crystals. Most organic molecules that form organic metals are planar, are of D_{2h} symmetry, and pack most efficiently in stacks like a deck of cards. The stacking direction corresponds to the long crystal axis mentioned above. Since in most organic metals approximately 50 percent of the molecules in a stack are charged, there is a definite ionic contribution to the lattice energy. However, there are still questions regarding cohesive forces in these salts (*2*)—for example, how much the metal-band electrons contribute to lattice binding energies, and whether these electrons contribute mostly by screening Coulombic repulsive forces (*3*).

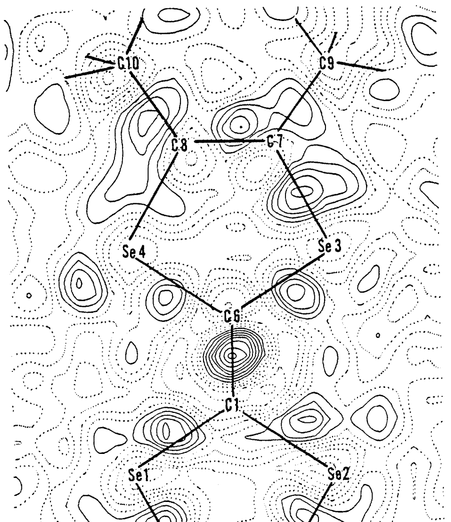

Fig. 1. Electron densities in the plane of a TMTSF molecule. Contours are 0.05 $e/\text{Å}^3$ per contour line starting at 0.05 $e/\text{Å}^3$; negative contours are shown by broken lines and the error is 0.05 $e/\text{Å}^3$ for all density maps.

The high conductivities observed along the stacking direction of organic metals are assumed to be due to the existence of intrastack bonding. In the first organic metal, tetrathiafulvalenium tetracyanoquinodimethanide (TTF-TCNQ), intermolecular intrastack bonding was inferred from comparisons of intermolecular intrastack distances in the neutral component molecules (for example, 3.62 Å in TTF-TTF and 3.45 Å in TCNQ-TCNQ) with the same intermolecular distances in TTF-TCNQ (3.47 Å in TTF-TTF and 3.17 Å in TCNQ-TCNQ). It was clearly of interest to determine the actual electron density distribution in an organic metal.

Recently, x-ray diffraction alone rather than combined x-ray and neutron diffraction has been used for experimental electron density studies (*4–7*). Experience has shown that to obtain meaningful electron density maps the crystals must be of excellent quality (*6, 7*). Such crystals were unavailable for the TCNQ-based metals (TTF-TCNQ, TSF-TCNQ, and so on) or TTF-based metals [$TTFI_n$, $TTF(SeCN)_n$], but were found for a family of the tetramethyltetraselenafulvalene (TMTSF) donor [$(TMTSF)_2X$, where X is an octahedral or tetrahedral complex univalent anion]. Wudl (*8*) reported that $(TMTSF)_2AsF_6$ forms nearly perfect crystals and suggested several interstack and intrastack selenium-selenium "bonding" interactions. The validity of these suggestions could be tested only through experimental electron density determinations.